SIMULATION OF UNSTEADY CAVITATION ON A 3D FOIL

R. Marcer, C. Audiffren

Principia, Athelia 1, 13705 La Ciotat Cedex, France

richard.marcer@principia.fr
charles.audiffren@principia.fr

Key words: 3D foil, cavitation, CFD, EOLE, KMT-VOF

Abstract. *Simulation of unsteady sheet cavitation on a 3D foil is concerned using the CFD EOLE code developed by Principia.*

The EOLE code is based on a multiphase Navier-Stokes KMT-VOF cavitation model (Kinematics and Mass Transfer VOF model). In this model, the cavitation dynamics is solved using the kinematics property of the VOF model, considering that the liquid/vapour interface moves with a velocity equal to the liquid velocity, and an additional thermodynamic effect introduced as a source term and characterizing mass transfer processes (vaporization and condensation).

Comparisons with experiments show the efficiency of the KMT-VOF model to simulate the main complex physical phenomena featuring of the unsteady sheet cavitating: variation of cavity length, break-up of the sheet cavity by 3D re-entrant jets, periodic dynamic shedding of cavities and repeatability of the periodic mechanism.

The results are obtained with a coarse mesh and a large time step, so requiring few CPU needs. Thus the model appears to be convenient in a context of industrial applications.

1 INTRODUCTION

Unsteady sheet cavitation which develops on propeller can be the cause of serious constraint such as noise, vibration and erosion. Some critical mechanisms characterize the physical phenomena: collapse of shedding cavities, induced pressure fluctuations, micro-jet impact on the wall.

If methods based on potential theory are efficient for attached sheet cavitation modelling, they fail to simulate unsteady cavitation with cavity shedding processes. Recent progresses have been done in CFD to simulate these complex phenomena.
Various methods can be found in the literature for calculating unsteady cavitation with URANS codes : mixture or single-fluid model using a barotropic equation artificially smoothed [1],[2], or based on the Rayleigh-Plesset (R-P) equation [3], two-fluids formulation of the conservation laws with use of the R-P equation for the calculation of the inter-phase transfer source terms [4],[5], eulerian formulation allowing to treat the vapour phase as a continuous vapour cloud with no-slip velocity between phases [6], model solving a volume fraction equation [7].
Other codes such as EOLE use a tracking interface methodology which is very well adapted for sheet cavitation modelling [9].
Recent works based on LES (Large Eddy Simulation) are giving promising results on academic applications due to their ability to represent detailed small turbulence scales [8]. But right now they can't be used for industrial applications because of too large CPU cost.

The Navier-Stokes URANS code EOLE, developed by Principia since 1991, has been extending for 15 years to simulate unsteady cavitating flows. The code includes two original cavitation models introducing a mass transfer source term in the VOF (Volume Of Fluid) model, basically only a pure kinematics model.
In EOLE, the VOF modeling can be based on a classical eulerian transport equation or on an improved eulerian-lagrangian model (SLVOF) developed by Principia [9],[10].
The code has been validated on a lot of industrial applications concerned by cavitation problems (see for example [11],[12],[13]).

In this paper, we are interested in simulation with EOLE of unsteady sheet cavitation on a 3D foil. An experiment campaign and detailed analysis were performed by Foeth and Terwisga to study cloud shedding mechanisms on a 3D twisted foil, for steady and unsteady operating conditions [14],[15]. Experimental results show that the cavitation development is fully 3D with a combination of a classical longitudinal re-entrant jet (as for 2D foils) and a spanwise component called side-entrant jet. The induced shedding cavity dynamics is visualized and shedding periods are extracted.
Comparisons between numerical and experimental results are presented in this paper.

2 THE NUMERICAL MODEL

2.1 Governing equations

Two incompressible viscous fluids with different densities separated by a moving interface are considered. The unsteady 3D Navier-Stokes equations for the two phase flows are then written in the following semi-conservative form, in curvilinear formulation:

$$\frac{1}{J}\frac{\partial W}{\partial t}+\frac{\partial F}{\partial \xi}+\frac{\partial G}{\partial \eta}+\frac{\partial H}{\partial \chi}=\frac{T}{J}+\frac{P}{J}$$

where F,G and H are the flux terms (convective, diffusive, pressure), T the surface tension source term, and P the gravity force :

$$F=\frac{1}{J}\begin{pmatrix}\rho\tilde{u}\\\rho\tilde{u}u+\xi_x p-\vec{\nabla}(\xi).\vec{\tau}_x\\\rho\tilde{u}v+\xi_y p-\vec{\nabla}(\xi).\vec{\tau}_y\\\rho\tilde{u}w+\xi_z p-\vec{\nabla}(\xi).\vec{\tau}_z\end{pmatrix};G=\frac{1}{J}\begin{pmatrix}\rho\tilde{v}\\\rho\tilde{v}u+\eta_x p-\vec{\nabla}(\eta).\vec{\tau}_x\\\rho\tilde{v}v+\eta_y p-\vec{\nabla}(\eta).\vec{\tau}_y\\\rho\tilde{v}w+\eta_z p-\vec{\nabla}(\eta).\vec{\tau}_z\end{pmatrix};H=\frac{1}{J}\begin{pmatrix}\rho\tilde{w}\\\rho\tilde{w}u+\chi_x p-\vec{\nabla}(\chi).\vec{\tau}_x\\\rho\tilde{w}v+\chi_y p-\vec{\nabla}(\chi).\vec{\tau}_y\\\rho\tilde{w}w+\chi_z p-\vec{\nabla}(\chi).\vec{\tau}_z\end{pmatrix}$$

$$W=\begin{pmatrix}0\\\rho u\\\rho v\\\rho w\end{pmatrix};T=\begin{pmatrix}0\\\sigma Rn_x\\\sigma Rn_y\\\sigma Rn_z\end{pmatrix};P=\begin{pmatrix}0\\0\\0\\-\rho g\end{pmatrix}$$

$$\tilde{u}=\xi_x u+\xi_y v+\xi_z w\;;\;\tilde{v}=\eta_x u+\eta_y v+\eta_z w\;;\;\tilde{w}=\chi_x u+\chi_y v+\chi_z w\;;\;J=\frac{\partial(\xi,\eta,\chi)}{\partial(x,y,z)}$$

$$\vec{\tau}_x=\overline{\overline{\tau}}.\vec{e}_x\quad\vec{\tau}_y=\overline{\overline{\tau}}.\vec{e}_y\quad\vec{\tau}_z=\overline{\overline{\tau}}.\vec{e}_z\quad\overline{\overline{\tau}}=-\frac{2}{3}\rho k\overline{\overline{I}}+(\mu+\mu_t)(\vec{\nabla}\vec{U}+\vec{\nabla}'\vec{U})$$

with (ξ,η,χ) the curvilinear coordinates, J the Jacobian of the coordinates transformation, $\vec{n}=(n_x,n_y,n_z)$ the normal vector to the interface, σ the surface tension coefficient and R the surface curvature. Additionally, (u,v,w) are the cartesian velocity components for each phase, $(\tilde{u},\tilde{v},\tilde{w})$ the contravariant velocity components, p the pressure, g the gravity, $\rho=C\rho_l+(1-C)\rho_v$ the density (with C the liquid volume fraction, ρ_l the liquid density and ρ_v the vapor density), μ the molecular viscosity, $\overline{\overline{\tau}}$ the sum of the viscous stress tensor and the Reynolds stress tensor, k the turbulent kinetic energy and μ_t the turbulent viscosity.

A k-ε model is used to simulate the turbulence of the flow.
The quantities k and ε are determined from convection-diffusion equations according to the well known Launder and Spalding formulation.

The model expresses the turbulent viscosity in terms of kinetic energy of turbulence k and its dissipation rate ε which is due to the velocity fluctuations:

$$\mu_t=C_\mu\rho\frac{k^2}{\varepsilon}$$

For cavitating flows, recent results showed that the isotropic k-ε model can introduce excessive dissipation responsible for an over-smoothing of the numerical results. For example, the re-entrant jet process which leads the shedding cavity mechanism, and more generally the unsteadiness of the flow, tends to be inhibited with the k-ε model, due to too large values of the eddy viscosity.

This problem can be overcome introducing an upper limit of the eddy viscosity. This one can be determined from a length scale of the turbulence which can be related with the dissipation rate ε by:

$$\varepsilon = \frac{C_\mu^{3/4}}{\kappa_p} \frac{k^{3:2}}{L}$$

with C_μ and κ_p constants of the model.

Fixing a characteristic length of the turbulence of the flow L_c, one can define a maximal value of the eddy viscosity with:

$$\mu_{t\max} = C_\mu \rho \frac{k^2}{\varepsilon_{\min}}$$

where $\varepsilon_{\min} = \frac{C_\mu^{3/4}}{\kappa_p} \frac{k^{3:2}}{L_c}$ is related with a given and imposed characteristic length of the turbulence.

Hence the eddy viscosity can be written:

$$\mu_t = \min\left(C_\mu \rho \frac{k^2}{\varepsilon}, \mu_{t\max} \right)$$

in which the first term is the classical one deduced from the solving of the k and ε equations and the second term, issued from a given characteristic length of the turbulence, prevents from having too much diffusion.

The flow solver is based on an original pseudo-unsteady system [16]. The pseudo-compressibility method used in EOLE differs from the classical method of Chorin. It is based on the idea of searching for pseudo-unsteady systems which, in the inviscid case, approach the exact unsteady compressible Euler equations as much as possible. For this purpose, pseudo-time derivative terms associated with a time-like variable τ called pseudo-time are introduced. The pseudo-time derivative term is constructed by replacing the true density by a pseudo-density, and the pressure is calculated as a given function, called pseudo equation of state, of this pseudo-density.

$$p^{n+1} = f(\tilde{\rho}^{n+1})$$

Considering a fully implicit second order scheme for the time discretization, considered in the second member of the equations, and the semi-discretized equations at the time level n+1, the curvilinear system is written:

$$\frac{1}{J} \frac{\partial \tilde{W}^{n+1}}{\partial \tau} + \left(\frac{\partial F}{\partial \xi} \right)^{n+1} + \left(\frac{\partial G}{\partial \eta} \right)^{n+1} + \left(\frac{\partial H}{\partial \chi} \right)^{n+1} = \frac{T^{n+1}}{J} + \frac{P}{J} + \frac{1}{J} \frac{3W^{n+1} - 4W^n + W^{n-1}}{2\Delta t}$$

with the dependent variables vector $\tilde{W} = \begin{pmatrix} \tilde{\rho} \\ \tilde{\rho}u \\ \tilde{\rho}v \\ \tilde{\rho}w \end{pmatrix}$

At each time step an iterative procedure (pseudo-time τ iteration) is operated so as $\dfrac{\partial \widetilde{W}^{n+1}}{\partial \tau} \to 0$ at convergence.

The code uses a finite volume method. The discretization in space is fully centered and artificial viscosity terms of fourth order are added to damp the numerical oscillations.
Integration in pseudo-time makes use of an explicit five stage Runge-Kutta scheme. An implicit residual smoothing operator is also applied following each stage of the Runge-Kutta scheme to improve stability.
The interest of local pseudo-time stepping is to greatly increase the convergence rate. This method is then particularly convenient to deal with multi-phase flows having phases with high density ratios.
The code runs on multi-processors machines, in MPI/OMP parallel mode.

2.2   KMT-VOF cavitation model

The numerical simulation of two-phase flows with phases separated by sharp interfaces, such as sheet cavitation (as opposite to cavitation bubble flows), requires simultaneous solutions of the Navier-Stokes equations in the two fluids and of the interface kinematics motion. Among the different kinds of interface tracking methods, the VOF model is one of the most efficient because of its ability to represent complex deformation of interfaces including break-up and reconnection.
The VOF method introduces a discrete function C whose value (included between 0 and 1) in each cell is the fraction of the cell occupied by the liquid. The fraction $1\text{-}C$ of the cell volume is occupied by vapour (cavitation).

The transport of the fraction C, so the motion of the interface in the fixed mesh, can be ensured by a classical eulerian method or a lagrangian method [9],[10].

For the eulerian method, a transport equation is solved for the VOF function:

$$\frac{\partial C}{\partial t} + div\left(C.\vec{V}\right) = 0$$

The inception of cavitation, so the passage of a non-cavitating one-phase flow to a 2-phase cavitating flow, is carried out when the pressure in the liquid flow reaches locally a critical threshold corresponding to the vapour pressure of the liquid phase. In this condition, the cavity is initialized in cells of the mesh which verify the vaporizing criterion.
Then, the motion of the interface is achieved by the kinematics part of the VOF (or SLVOF) model, with a velocity equal to the normal velocity of the liquid, coupled with a thermodynamic part characterizing the mass transfer process (vaporization and condensation).

Two cavitation models, developed by Principia, have been implemented in EOLE to simulate the mass transfer processes on liquid-vapour interfaces [11],[12].

In this study we used the KMT-VOF model (Kinematics and Mass Transfer VOF model) in which two source terms are considered to account for the mass transfer between phases: S_v and S_c respectively for the vaporization and the condensation.

These terms are active depending on the pressure values in the fluid. For vaporization, S_v gives the mass transfer imposed for liquid cells of the mesh having a pressure lower than the cavitation pressure. On the opposite, for condensation S_c gives the mass transfer imposed for vapour cells of the mesh having a pressure higher than the cavitation pressure.
They have the following form:

$$S_v, S_c = f\left(\frac{P_v - P}{\Delta P}\right)$$

Considering that for a given cell, C represents the fraction occupied by the denser fluid. Hence the VOF equation including the mass transfer process is written:

$$\frac{\partial C}{\partial t} + div\left(C.\vec{V}\right) = S_c - S_v$$

The solving of this equation means a correction of the liquid-vapour position computed by the VOF (or SLVOF) method, and representative of the purely kinematic part of the cavitating flow, in order to take into account mass transfer effects. So the "kinematic" VOF field is modified in such a way that the interface is constrained to fit the vapour pressure isobar and therefore the pressure of the liquid phase is higher than the vapour pressure, and on the opposite the pressure of the vapour remains below the vapour pressure.

3   DELFT TWIST MODELLING

The 3D Delft hydrofoil (Figure 1) has a chord length of L=150mm, a span of 300mm and a span wise varying angle of attack with a maximum 11° at midspan and 0° at the tunnel walls.
In the study, a -2° rotation of the foil is considered, thus the angle of attack is 9° at midspan and -2° at the tunnel wall
Due to symmetry conditions with respect to the midspan, only half of the geometry is considered in the numerical model.
The extension of the mesh is 2L in front of the leading edge and 3L behind trailing edge. Two blocks based on an H topology are used with a local wall refinement allowing correct y+ values required for the wall function of the k-ε model (Figure 2).
The number of cells is half a million which is quite small.

The boundary conditions are:

- Foil : no-slip condition
- tunnel wall (lateral, bottom and top) : slip condition
- midplan of the foil : symmetry condition

- Inlet : uniformed velocity = 6.97 m/s
- Outlet : uniformed pressure = 29 kPa

The density and the dynamic viscosity of the liquid are respectively 1000 km/m^3 and 0.0012 kg/ms.

The cavitation number in this condition is 1.07.

The time step of the simulation is 1ms. The shedding periods highlighted in experiments being of about 50ms long, it means that only 50 time steps will be considered for the discretization of a shedding period.

The total time of the simulation is about 15 shedding periods.
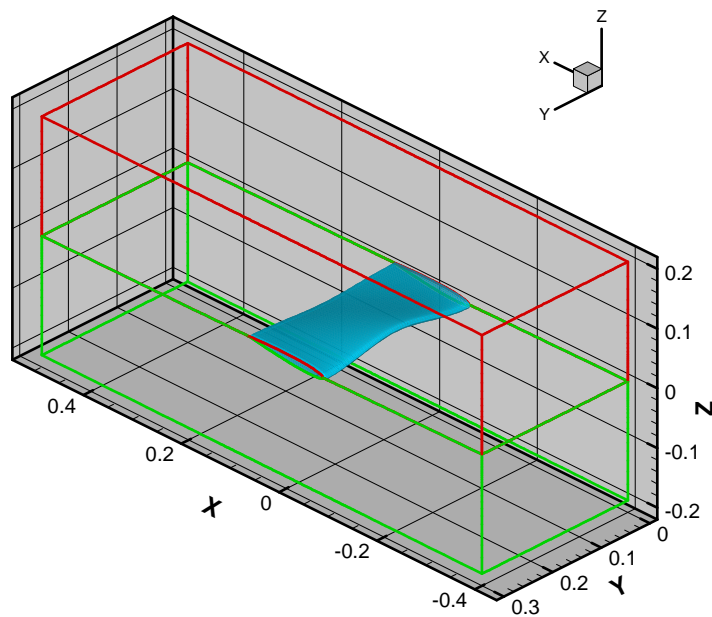
Figure 1: view of the 3D twisted hydrofoil
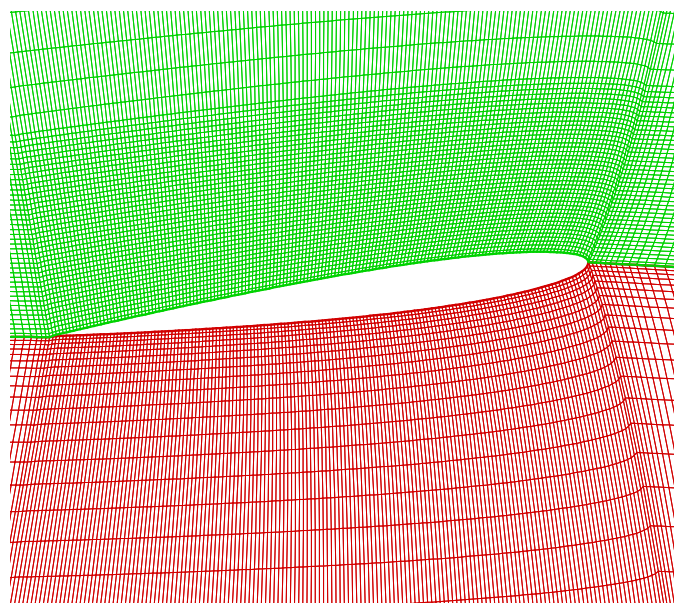
Figure 2: view of the mesh

4   RESULTS

4.1   Sheet cavity dynamics

As for experimental visualizations, numerical results show that the cavitation pattern is periodic whereas the operating flow conditions (velocity and pressure) are steady.
Figure 3 shows different steps of a shedding period obtained with the numerical model. The liquid/vapour interface is represented with an iso-surface of VOF=0.5.
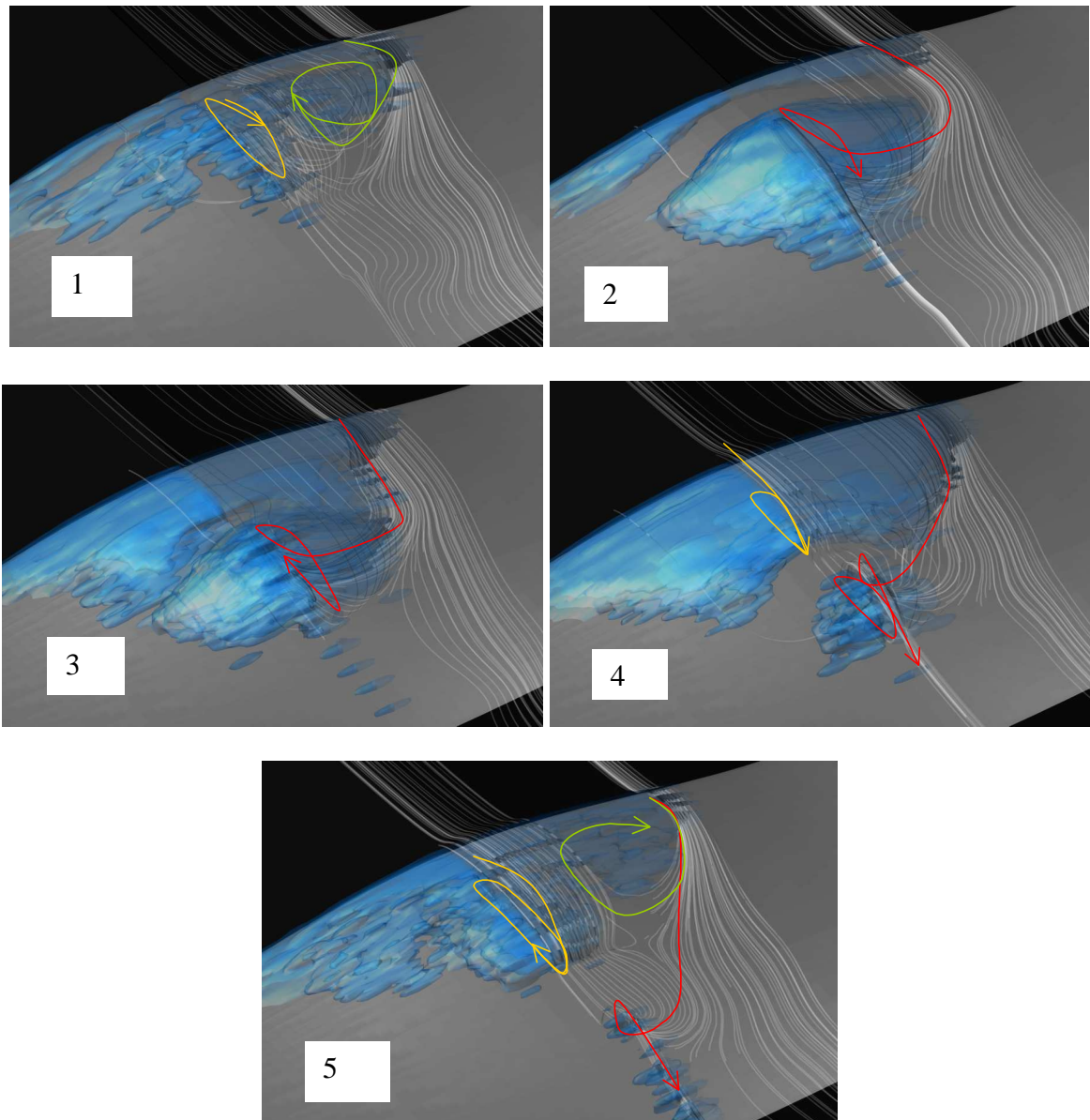

Figure 3: numerical results – description of the 3D shedding mechanism

1) Two independent vortices develop, a spanwise one parallel to the wall, inducing a side-entrant jet (in green) and a vertical longitudinal vortex in yellow at the mid-plan of the foil from which a re-entrant jet is issued.

2) So, a primary shedding is induced by combination of these two jets which have merged into a single one (in red).

3) A new attached sheet cavity takes place at the leading edge and is convected by the incident flow whereas the shedding cavity moves downstream.

4) The size of the attached sheet cavity reaches its maximum length. A new re-entrant jet (in yellow) is generated at mid-plan of the foil. It detaches the sheet cavity from the wall and thus initialises the next shedding mechanism. The size of the shedding cavity decreases and the associated vortex intensity (in red) is damped.

5) A new side-entrant jet (in green) occurs whereas the intensity of the re-entrant jet increases (in yellow). The shedding cavity induced by the previous vortex (in red) is spread out downstream. Then the same mechanism described in the step 1 takes place.

This computed shedding cavity process has been observed in experiments as well. Figure 4 shows snapshots of the unsteady cavitation development obtained with the numerical model and in experiments, at the same instants. The comparisons highlight very comparable mechanisms on a shedding period.
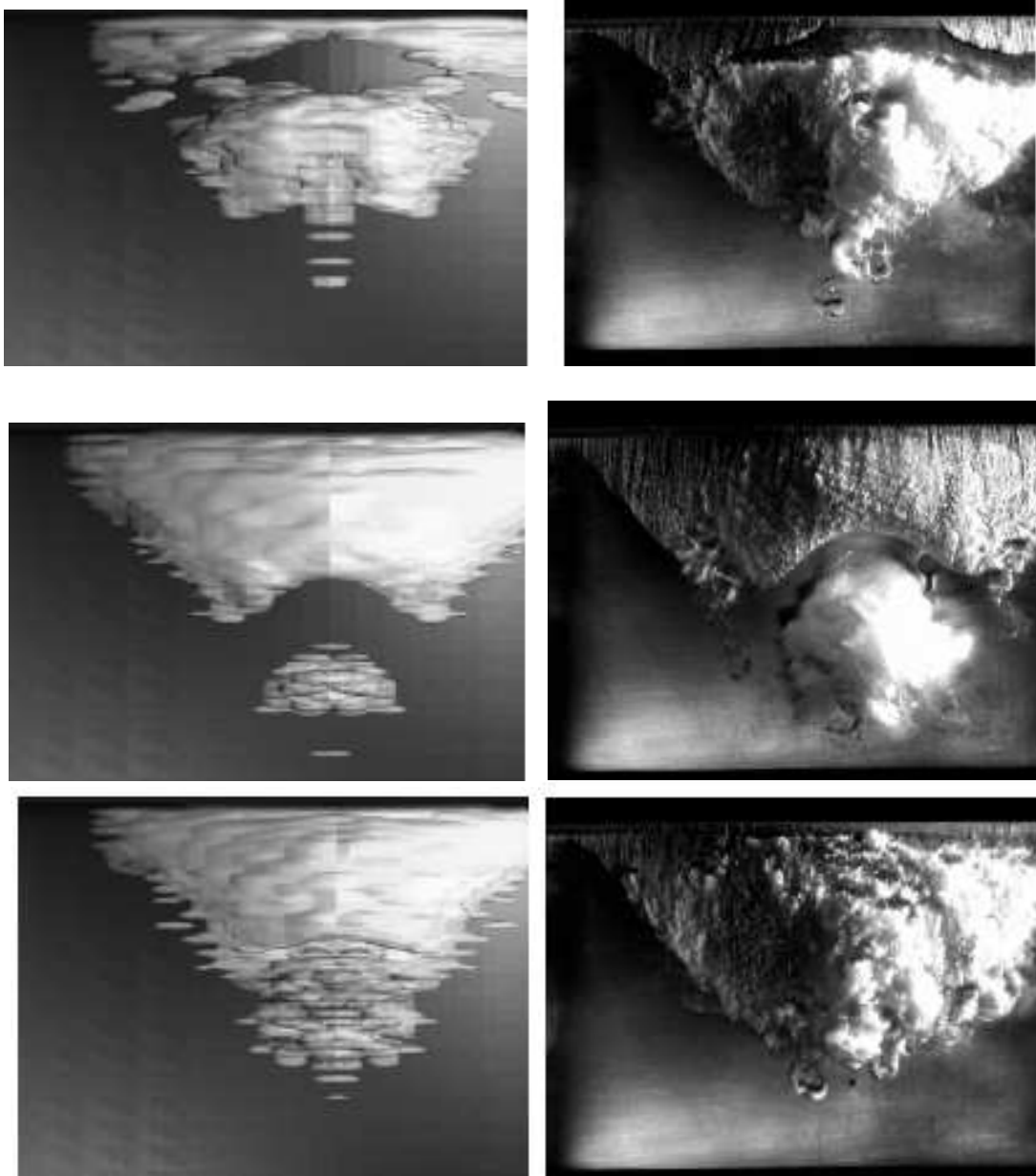
Figure 4 : comparison EOLE (left) / measurements (right) [14] of the cavity pattern at different instants – view from above of the suction side

Particularly, the numerical model put into evidence the observed re-entrant and side-entrant jets (Figure 5).
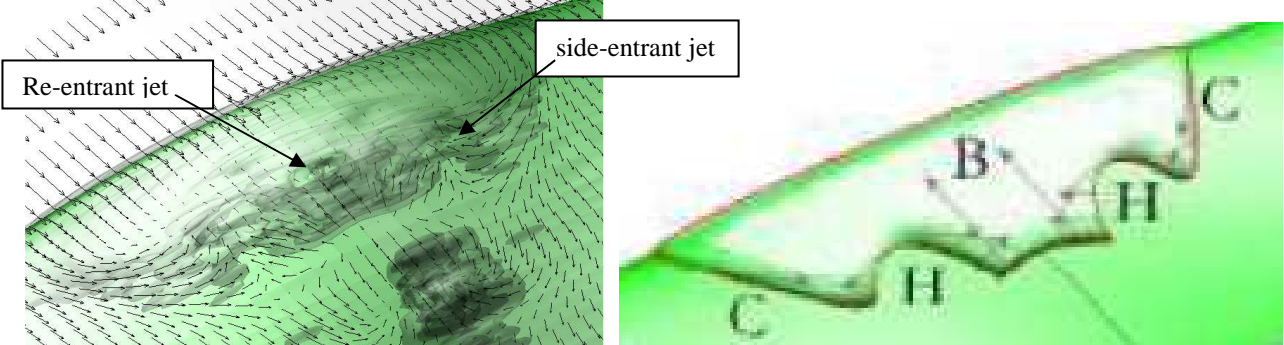

Figure 5 : Re-entrant (B) and side-entrant jets (H) – comparison EOLE / sketch of the observed side and re-entrant jet [15]
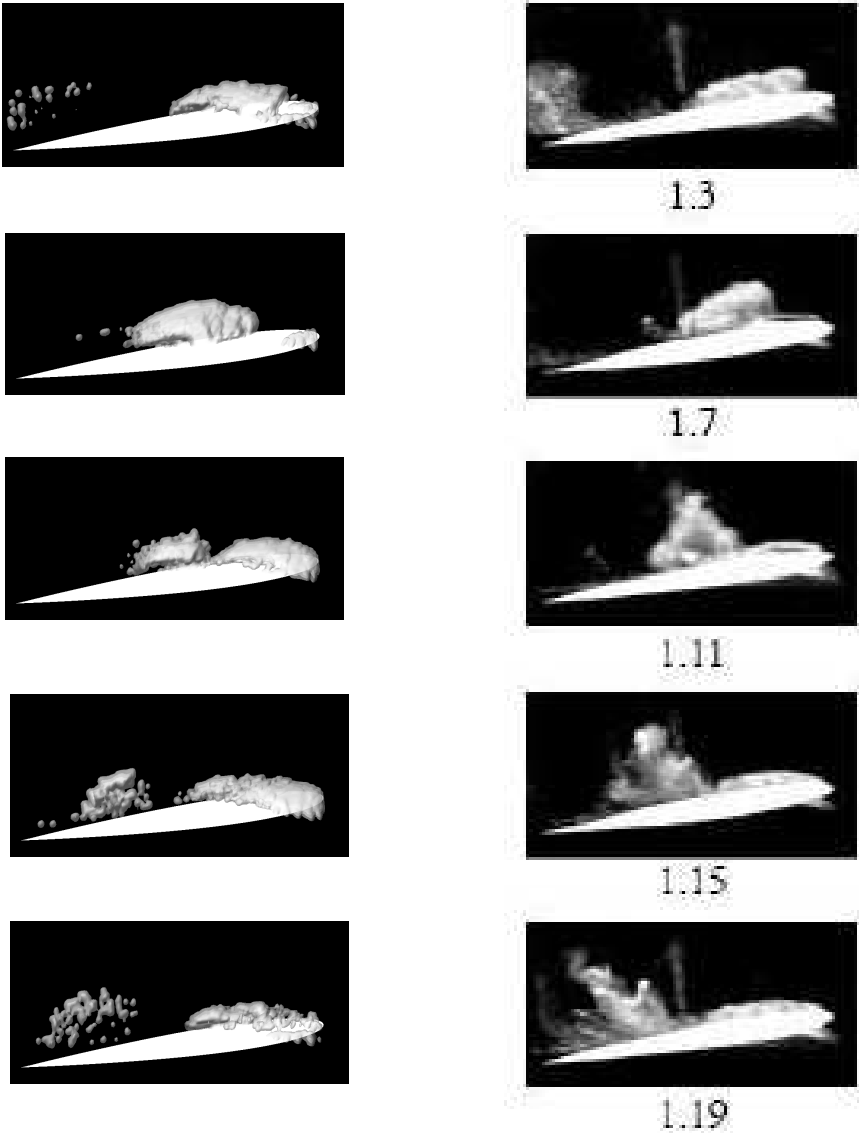

Figure 6: view from the side where the central plane of the foil is visible on the white section but the cavitation appears in 3D (and not on the 2D central plan) - comparisons of cavitation pattern between EOLE (left) and experiments (right) [14] during a shedding period

Figure 6 shows a comparison of the cavitation development at the midplan of the foil, within one period of the shedding cycle. The time interval is equal between successive images and each numerical and experimental snapshot to compare is given at the same time. Both results yield very similar behaviour of the shedding dynamics. The sheet cavity extends from the leading edge and is cut off by an up-ward re-entrant jet coupled with the side-entrant jet (which of course is not visible on these 2D pictures). Both attached sheet cavity and shedding cavity lengths are remarkably well reproduced by the numerical code.

The repeatability of the shedding cavity cycle is put into evidence with the numerical model Figure 7). Four consecutive periods are shown and, for each cycle, five snapshots are given at the same time. Even if not specific refined numerical parameters are considered in this calculation (coarse mesh, large time step) - parameters which may be required for most of classical cavitation models - the VOF free surface method coupled with the KMT cavitation model turns out very efficient to capture the repeatable high dynamic cavitation processes.
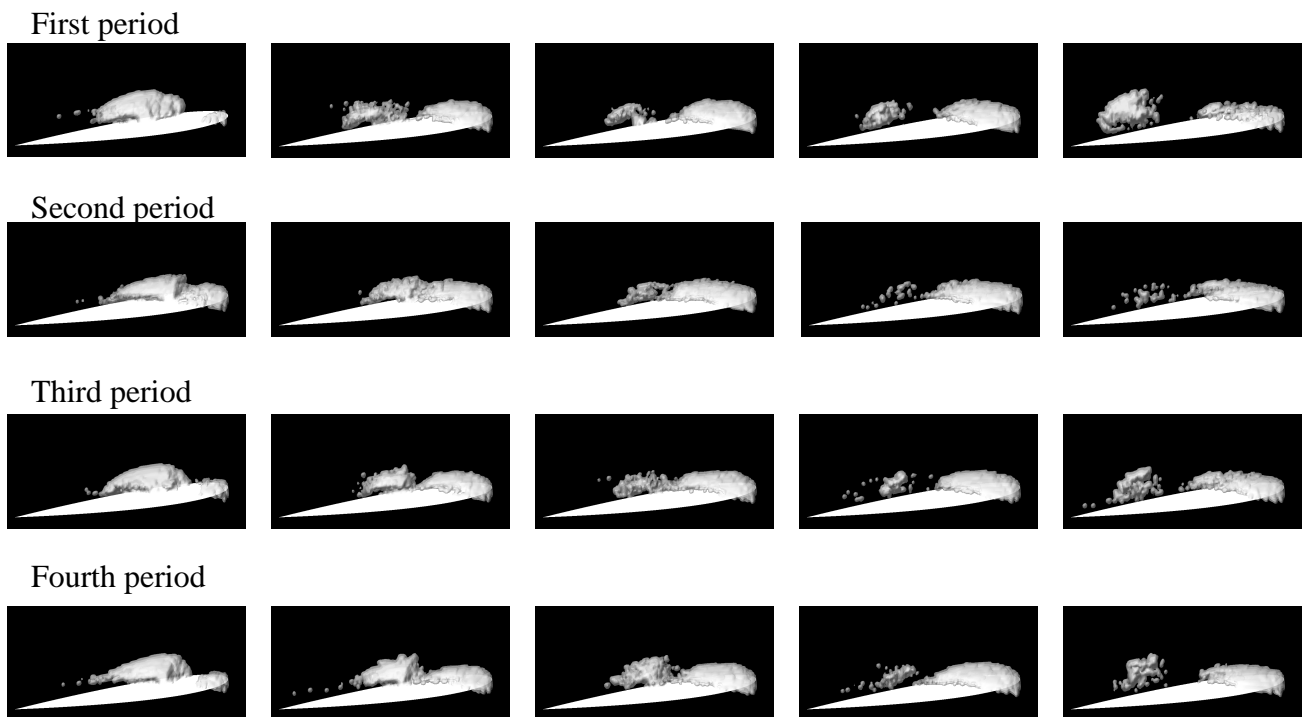
First period

Second period

Third period

Fourth period

Figure 7: EOLE results – four consecutive shedding periods

4.2   Lift force and shedding frequency

The time history of the lift force shows a periodic variation of the load (Figure 8). The deduced time-averaged lift force is ≈422N, so about 8% lower than the measured one ≈455N
The shedding frequency is computed from a spectral analysis of the unsteady lift force. A main frequency is extracted at 18 Hz (Figure 9). Experiment highlights a frequency of about 21 Hz considering a 15% uncertainty.

Strouhal numbers can be compared ($St = \dfrac{fl}{V}$ with f the shedding frequency, l the maximal cavity length on aperiod and V the incident fluid velocity). The obtained values are:

- 0.185 for experiments
- 0.188 for the numerical model

These values are very close but the comparison remains qualitative due to the fact that the maximal cavity length is only deduced from visual inspection.
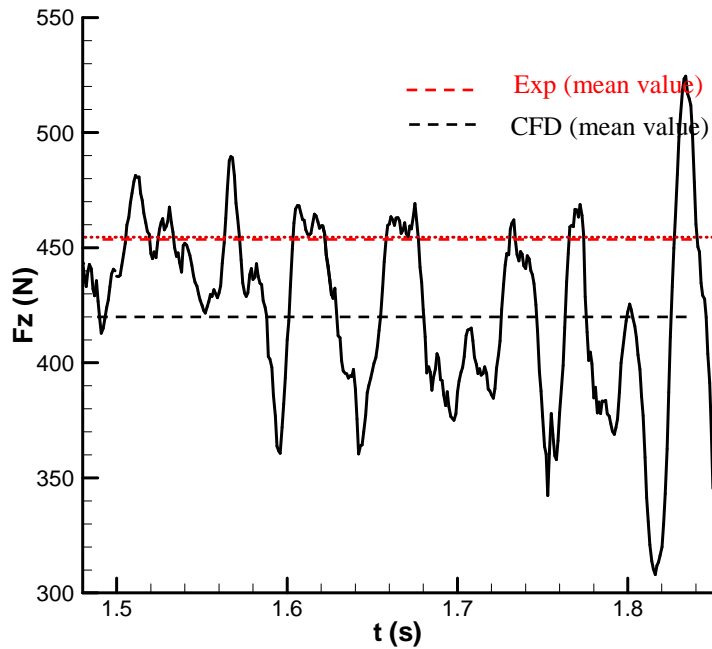

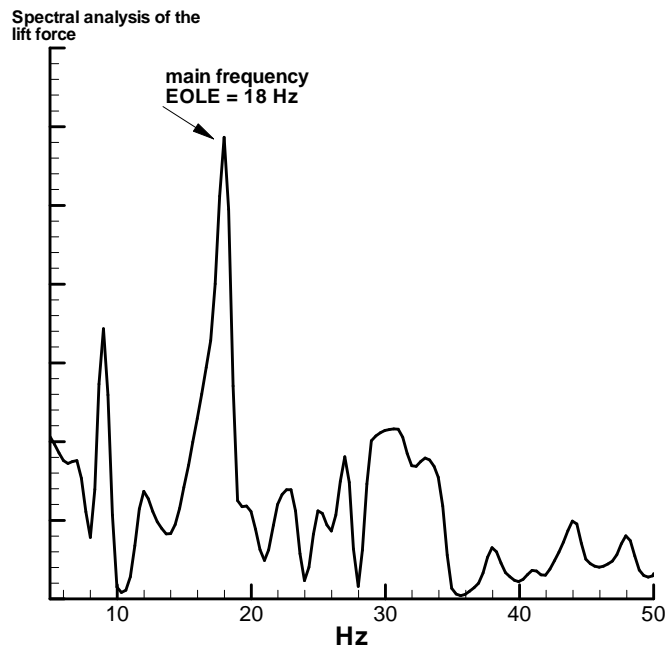**Figure 8: time evolution of the lift force**

Figure 9: Spectral analysis of the lift force

5   CONCLUSIONS

Simulations with EOLE of unsteady sheet cavitation on the 3D Delft twisted foil were carried out and compared with experiments. The results show the efficiency of the KMT-VOF model to simulate the main complex physical phenomena featuring that kind of cavitating flow: break-up of the attached sheet cavity by the combination of 3D re-entrant and side-entrant jets, cavity dynamic shedding, repeatability of the periodic mechanism.

Moreover, the results are obtained with a coarse mesh and a large time step, so requiring few CPU needs. Thus the model appears to be convenient in a context of industrial applications.

REFERENCES

[1] Schmidt and Corradini, Analytical prediction of the exit flow of cavitating orifice, Atomization and Sprays, vol. 7, pp. 603-616, 1997.

[2] Delannoy B., Kueny H., two phase flow approach in unsteady cavitating modelling, ASME Cavitation and Multiphase flow forum, 98:153-158, 1990.

[3] Kubota A., Kato H., Yamagushi H., A new modelling of Cavitating flows : a numerical study of unsteady cavitation on a hydrofoil section, J. Fluid Mech., Vol. 240, pp. 59-96, 1992.

[4] Tatschl, Künsberg Sarre, Alajbegovic and Winklhofer (2000): "Diesel spray break-up modelling including multidimensional cavitating nozzle flow effects", ILASS Darmstadt, september 2000.

[5] Cokljat, Ivanov and Vasquez (1998): "Two-phase model for cavitating flows", 3rd Int. Conference on multiphase flows, ICMF'98, Lyon.

[6] Xu, Bunnell and Heister (2001): "On the influence of internal flow structure on performance of plain-orifice atomizers", Atomization and sprays, vol. 11, pp 335-350.

[7] Kunz R., Boger D., Chyczewski T., Stinebring D. and Gibeling H., Multi-phase CFD Analysis of Natural and Ventilated Cavitation around Submerged Bodies, 3rd ASME/JSME Joint Fluids Engineering Conference, USA, 1999.

[8] Huuva T., Large eddy simulation of cavitating and no-cavitating flow, PhD thesis, Chalmers University of Technology, Sweden, 2008.

[9] S.Guignard, R.Marcer, V.Rey, C.Kharif, P.Fraunié, Solitary wave breaking on sloping beaches : 2D two phase flow numerical simulation by SL-VOF method, Eur. J. Mech. B, Fluids 20 (2001) 57-74.

[10] B.Biausser, R.Marcer, S.Guignard, P.Fraunié, *3-D two phase flows numerical simulations by SL-VOF method,* Int. J. For Numer. Meth. Fluids 2004 ; 45 :581-604.

[11] R.Marcer, P.Le Cottier, H.Chaves, B.Argueyrolles, C.Habchi, B.Barbeau, A validated Numerical Simulation of Diesel Injector Flow Using a VOF method, SAE Paper 2000-01-2932, Baltimore Octobre 2000.

[12] R.Marcer, J.M.Legouez, L.Diéval, M.Arnaud, Improvement of a VOF Method for Multiphase Flows, Third Inter. Conf. On Multiphase Flow, Lyon, 1998.

[13] R. Marcer, C. Dassibat, B. Argueyrolles, Simulation of two-phase flows in injectors with the CFD code EOLE, Paper ID ILASS08-A060, ILASS, Sept. 2008.

[14] Foeth E.J., The structure of three-dimensional sheet cavitation, PhD thesis, Technical University of Delft, The Netherlands, 2008.

[15] E.J. Foeth, T.V. Terwisga, An attached cavity of the three-dimensional hydrofoil, Sixth Int. Symp. on Cavitation, CAV2006, Wageningen, Sept. 2006.

 [16] C.deJouëtte, H.Viviand, S.Wornom, J.M. LeGouez, Pseudo compressibility method for incompressible flow calculation, 4th International Symposium on Comp. Fluid Dyn. Of California at Davis - sept. 9-12, 1991.

AKNOWLEDGMENTS